Performance Optimization of Au-Free Lateral AlGaN/GaN Schottky Barrier Diode With Gated Edge Termination on 200-mm Silicon Substrate

Jie Hu, *Student Member, IEEE*, Steve Stoffels, Silvia Lenci, Benoit Bakeroot, Brice De Jaeger, Marleen Van Hove, Nicolò Ronchi, Rafael Venegas, Hu Liang, Ming Zhao, Guido Groeseneken, *Fellow, IEEE*, and Stefaan Decoutere

***Abstract*— In this paper, a further leakage reduction of AlGaN/GaN Schottky barrier diodes with gated edge termination (GET-SBDs) has been achieved by optimizing the physical vapor deposited TiN as the anode metal without severe degradation of ON-state characteristics. The optimized GET-SBD multifinger power diodes with 10 mm anode width deliver ∼4 A at 2 V and show a median leakage of 1.3 μA at 25 °C and 3.8 μA at 150 °C measured at a reverse voltage of −200 V. The temperature-dependent leakage of Si, SiC, and our GaN power diodes has been compared. The breakdown voltage (BV) of GET-SBDs was evaluated by the variation of anode-to-cathode spacing (L_{AC}) and the length of field plate. We observed a saturated BV of ∼600 V for the GET-SBDs with L_{AC} larger than 5 μm. The GET-SBD breakdown mechanism is shown to be determined by the parasitic vertical leakage current through the 2.8 μm-thick buffer layers measured with a grounding substrate. Furthermore, we show that the forward voltage of GET-SBDs can be improved by shrinking the lateral dimension of the edge termination due to reduced series resistance. The leakage current shows no dependence on the layout dimension L_G (from 2 to 0.75 μm) and remains at a value of ∼10 nA/mm. The optimized Au-free GET-SBD with low leakage current and improved forward voltage competes with high-performance lateral AlGaN/GaN SBDs reported in the literature.**

***Index Terms*— 200-mm substrate, AlGaN/GaN, Au-free, edge termination, leakage reduction, Schottky barrier diode (SBD), TiN.**

I. Introduction

OVER the last few years, electronic devices based on AlGaN/GaN heterojunction have emerged as promising candidates for high-power switching applications due to the superior material properties compared with conventional silicon [1]–[5]. The wide bandgap nature of GaN-based electronic devices and the high mobility and electron density of the 2-D electron gas (2DEG) at the AlGaN/GaN heterointerface lead to a high-power figure-of-merit (FOM) $BV^2/R_{ON,SP}$ and enable power conversion with higher efficiency [6]. To enable low-cost production of GaN-based devices, many research groups have been developing AlGaN/GaN epi-layers on large-area silicon substrates [7]. Recently, the fabrication of high-performance AlGaN/GaN high electron mobility transistors and Schottky barrier diodes (SBDs) with a Au-free CMOS-compatible process flow on a 200-mm Si substrate has been a major breakthrough for the realization of efficient high-power devices at low manufacturing cost [4], [8].

In efficient power converters, the GaN-based SBD is required to have a low leakage current in the OFF-state and a low forward voltage drop in the ON-state, thus minimal static power loss of the diode can be obtained [9]. Partial or full AlGaN barrier recess in the anode region has been reported to increase the forward current and lower the forward voltage drop [3], [9]. Furthermore, AlGaN/GaN SBDs with gated ohmic anode structure have been proposed to achieve low turn-ON voltages [10]. Various designs of field-plates and edge terminations in lateral and vertical GaN-based SBDs have been reported to suppress the OFF-state leakage current [9], [11], [12]. Matioli *et al.* [13] presented a lateral AlGaN/GaN SBD with a 3-D anode structure, where an integration of a trigate MOS structure with a Schottky junction is designed, demonstrating an ultralow leakage of 260 pA/mm and a turn-ON voltage of 0.85 V. Among those promising AlGaN/GaN SBD architectures, typical high work-function (ϕ_m) Ni/Au or Pt-based metals were used for the fabrication of the Schottky contacts [3], [6], [10], [12], [13]. This hinders the high-volume production of those high-performance devices in existing CMOS-compatible processing lines because of their limited dry-etch capability [14].

In [4], we have demonstrated an architecture of the AlGaN/GaN SBD with gated edge termination (GET-SBD) in Au-free technology and obtained significant diode leakage reduction and good ON-state characteristics. The embedded edge termination in the anode trench enables the reduction of the peak E-field at the anode edge; thus, a low leakage current was obtained in AlGaN/GaN SBDs [9]. Since the

Manuscript received October 23, 2015; revised December 15, 2015; accepted January 5, 2016. Date of publication January 20, 2016; date of current version February 23, 2016. This work was supported by the imec's Industrial Affiliation Program through the GaN Project. The review of this paper was arranged by Editor W. Tsai.

J. Hu and G. Groeseneken are with imec, Leuven 3001, Belgium, and also with the Department of Electrical Engineering–Microelectronics and Sensors, KU Leuven, Leuven 3001, Belgium (e-mail: jie.hu@imec.be; guido.groeseneken@imec.be).

S. Stoffels, S. Lenci, B. De Jaeger, M. Van Hove, N. Ronchi, R. Venegas, H. Liang, M. Zhao, and S. Decoutere are with imec, Leuven 3001, Belgium (e-mail: steve.stoffels@imec.be; silvia.lenci@imec.be; brice.dejaeger@imec.be; marleen.vanhove@imec.be; nicolo.ronchi@imec.be; rafael.venegas@imec.be; hu.liang@imec.be; ming.zhao@imec.be; stefaan.decoutere@imec.be).

B. Bakeroot is with imec, Leuven 3001, Belgium, and also with the Centre for Microsystems Technology, Department of Electronics and Information Systems, Ghent University, Ghent 9052, Belgium (e-mail: benoit.bakeroot@imec.be).

Color versions of one or more of the figures in this paper are available online at http://ieeexplore.ieee.org.

Digital Object Identifier 10.1109/TED.2016.2515566

0018-9383 © 2016 IEEE. Personal use is permitted, but republication/redistribution requires IEEE permission.
See http://www.ieee.org/publications_standards/publications/rights/index.html for more information.

Schottky barrier height (SBH ϕ_B) is an important parameter determining the diode characteristics, the selection of high work-function Au-free metals for anode electrode can potentially improve the OFF-state characteristics and optimize the performance of the AlGaN/GaN SBDs [15].

In this paper, we extensively study the impact of anode metal and layout parameters on the diode's OFF- and ON-state characteristics. We used two different types of TiN, a standard physical vapor deposited (PVD) TiN and a PVD TiN with ionized metal plasma source (IMP TiN), as the anode metal in intimate contact with the AlGaN barrier. The IMP TiN showed a high-ϕ_m, which allows a further reduction in the leakage current of the AlGaN/GaN GET-SBD. The leakage reduction by optimizing the TiN has been confirmed on small diodes and multifinger power diodes with total anode width of 10 mm. The diode forward voltage is found to scale down with the reduction of the length of edge termination without sacrificing the leakage characteristics. The benchmarking of the diode leakage current and forward voltage shows that our optimized GET-SBDs demonstrate very competitive performances with those of reported lateral AlGaN/GaN SBDs, which are mostly fabricated with Ni/Au-based technologies [3], [6], [10], [12], [13].

II. Experimental Details

A. Epi-Structure and Device Processing

AlGaN/GaN heterostructure layers were grown on 200-mm silicon wafers by metalorganic chemical vapor deposition (MOCVD). The epi-stack consists of a 10-nm $Al_{0.25}Ga_{0.75}N$ barrier, a 150-nm GaN channel layer, a 2.8-μm C-doped AlGaN buffer as the back-barrier, and a 200-nm AlN nucleation layer on p-type Si(111) substrates. The passivation capping layer of the wafers was 5 nm *in situ* MOCVD Si_3N_4. The surface of the entire stack was then encapsulated by a 140-nm Si_3N_4 layer by means of rapid thermal chemical vapor deposition. The removal of the Si_3N_4 passivation layer in the anode region was performed by SF_6 dry-etching. The AlGaN barrier recess was performed with an atomic layer etching process. After recess, the 5-nm AlGaN barrier was left in the anode region. To form an edge termination, the 15-nm Si_3N_4 layer was deposited inside the anode trench by means of plasma-enhanced atomic layer deposition. The center region was opened to allow the formation of a Schottky contact on the top of the AlGaN barrier. Before the deposition of the anode metal, an *in situ* N_2 plasma cleaning treatment of the anode area was done to clean the AlGaN surface [16]. The Au-free anode metal stack is composed of 20-nm TiN/20-nm Ti/250-nm Al/20-nm Ti/60-nm TiN. An Au-free metal stack of Ti/Al-based metals was deposited for the cathode contact formation, which was annealed at 550 °C [4]. A schematic of the AlGaN/GaN SBD with gated edge termination (GET-SBD) is shown in Fig. 1(a). Two-level anode FPs are fabricated on the Si_3N_4 passivation layers toward the cathode. The layout design of the GET-SBD is shown in Fig. 1(b). The Schottky contact length (L_{SC}), the anode finger width, and the anode-to-cathode distance (L_{AC}) were 6, 100, and 5 μm, respectively. A cross-sectional SEM image of the anode region in GET-SBD is shown in Fig. 1(c), presenting L_G of 1.5-μm gated edge termination (GET) and two-level anode metal FPs. The conventional AlGaN/GaN SBD (without edge termination and without AlGaN barrier recess) was also processed as a reference, and the two-level FP structure was fabricated as well in the reference SBD.

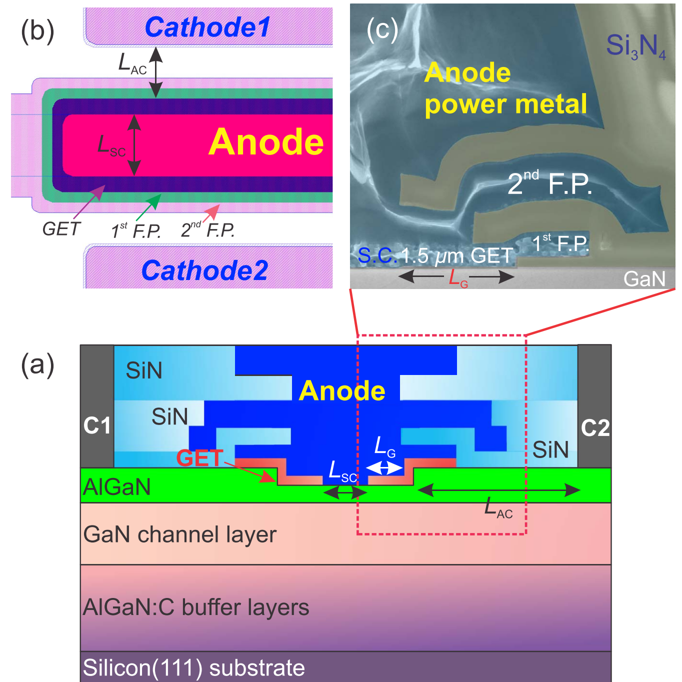

Fig. 1. (a) Schematic cross section of the AlGaN/GaN GET-SBD and two-level FPs. (b) Layout design of the GET-SBD. (c) Cross-sectional SEM image of the anode region in GET-SBD.

B. Optimization of TiN as Anode Metal

Concerning the bottom 20-nm TiN layer, standard PVD TiN (at 23 °C) and IMP PVD TiN (at 350 °C) were used separately on two otherwise identical wafers. For the deposition of IMP TiN, an inductively coupled Ar/N_2 plasma was used to ionize the sputtered atoms at a relatively high temperature. The crystallographic orientation of PVD TiN and IMP TiN was examined by the grazing incidence X-ray diffraction (GIXRD) with spectra shown in Fig. 2(a). It was found that IMP TiN predominantly consists of (200) crystallites (a peak at 42.5°) compared with mixed grain orientations in standard PVD TiN [17]. The difference can be related to the difference in deposition temperature because metal tends to grow in a preferred orientation to obtain a stable crystal structure at high deposition temperatures [18]. The deposition details and material properties of these two TiN metals are further summarized in Table I. It was reported that the work-function of metals is dependent on the crystallographic orientation [19]. Capacitance–voltage (C–V) measurements have been performed at 100 kHz on conventional AlGaN/GaN SBD and GET-SBD with IMP TiN and standard PVD TiN, respectively [in Fig. 2(b)]. A positive V_{TH} shift (~200 mV) is observed in the SBD and GET-SBD with IMP TiN compared with devices using PVD TiN, this indicates a higher ϕ_m for IMP TiN compared with standard PVD TiN.

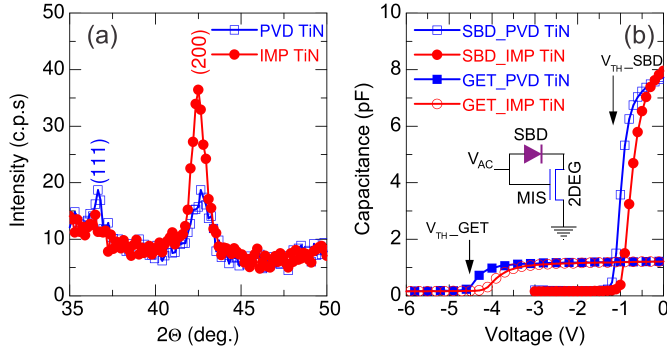

Fig. 2. (a) GIXRD spectra of the standard PVD TiN and the IMP TiN. (b) Capacitance–voltage (C–V) measurements on conventional AlGaN/GaN SBD and GET-SBD with IMP TiN and standard PVD TiN, respectively. The V_{TH} of SBD and GET-SBD is shifted positively with a value of ∼200 mV with IMP TiN.

TABLE I

DEPOSITION DETAILS AND PROPERTIES OF STANDARD PVD TiN AND IMP TiN

	Temperature (°C)	Thickness (nm)	Crystal orientation
PVD TiN	350	20	(200) and (111)
IMP TiN	23	20	(111)

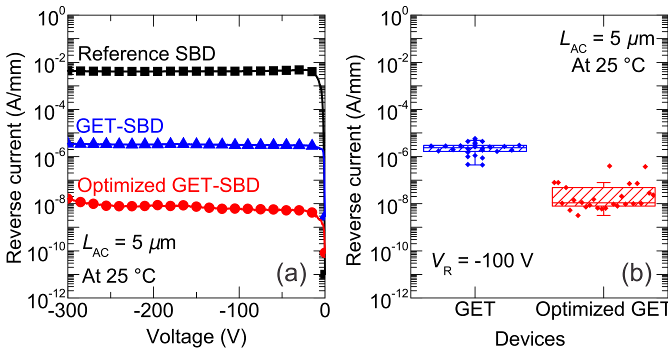

Fig. 3. (a) Typical OFF-state characteristics of the GET-SBD (labeled as GET-SBD1) and the one with optimized TiN anode metal (labeled as GET-SBD2) measured down to V_R of −300 V, the leakage of a reference AlGaN/GaN SBD is also shown. (b) Statistical plot of room-temperature leakage current (at V_R of −100 V) for GET-SBD1 and GET-SBD2.

III. RESULTS AND DISCUSSION

A. Leakage Optimization With IMP TiN

As displayed in Fig. 3(a), the leakage current of conventional SBD, GET-SBD with standard PVD TiN (labeled as GET-SBD1), and GET-SBD with IMP TiN (GET-SBD2) is measured (at 25 °C) down to a reverse voltage (V_R) of −300 V. The conventional AlGaN/GaN SBD (with PVD TiN as the anode metal) suffers from high leakage due to electron tunneling through the AlGaN barrier layer in the lateral depletion region [9], though a 1-μm-long FP was fabricated on the 140-nm-thick Si_3N_4 layer. In the GET-SBD, the edge termination (15-nm Si_3N_4) pinches off the 2DEG channel effectively and redistributes the electric field in the vicinity of the Schottky contact [4], [9]. With the same anode metal of PVD TiN, GET-SBD1 shows three-order-of-magnitude reduction in leakage compared with the conventional SBD. When a

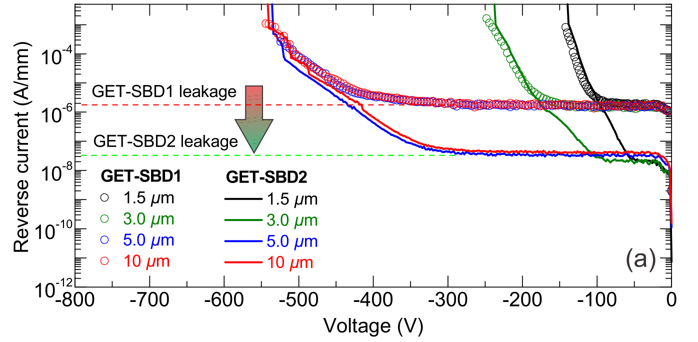

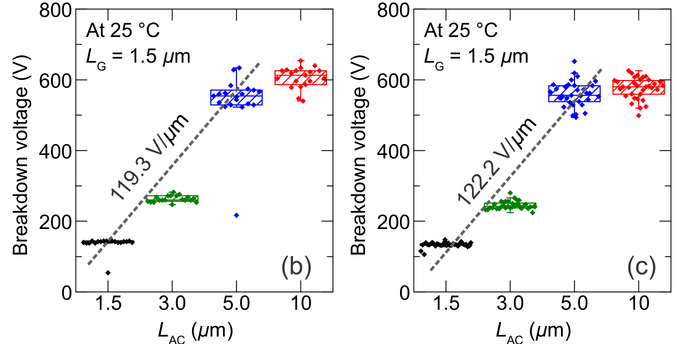

Fig. 4. (a) Typical leakage and breakdown characteristics of the GET-SBDs and optimized GET-SBDs with a variation of anode-to-cathode spacing L_{AC}. The statistical plots of BV (at current level of 5 mA/mm) in GET-SBD1 and optimized GET-SBD2 with four different L_{AC} are shown in (b) and (c), respectively.

thicker Si_3N_4 is used in the edge termination, the V_{TH} of the GET structure will shift in the negative direction. This can lead to an increase of the leakage. By combining a high-ϕ_m IMP TiN and an edge termination in GET-SBD2, a higher SBH and lower E-field can be obtained simultaneously, resulting in a stronger blocking capability for the leakage. This yields a 5 to 6 orders of magnitude leakage reduction compared with the conventional devices with PVD TiN. In Fig. 3(b), the statistical leakage value over the 200-mm wafers (at V_R of −100 V) of GET-SBD1 and optimized GET-SBD2 with IMP TiN is shown. It confirms that the leakage current can be further reduced with a high ϕ_m IMP TiN as anode metal. The optimized GET-SBD2 shows a median leakage value of 10.8 nA/mm compared with 2.39 μA/mm in the case of GET-SBD1 with standard TiN as the anode metal.

To evaluate the breakdown voltage (BV), OFF-state measurements on both GET-SBD1 and optimized GET-SBD2 with a variation of anode-to-cathode spacing L_{AC} (from 1.5 to 10 μm) are performed. As presented in Fig. 4(a), the diode leakage current (prior to the diode breakdown or buffer breakdown) is independent of L_{AC} in both GET-SBDs due to the function of the gated edge termination. This observation is different from the results reported in [10] and [20], where a L_{AC}-dependent leakage characteristics were shown. The difference in leakage current between the GET-SBD1 and the optimized GET-SBD2 is further shown in Fig. 4(a). The BV of these two GET-SBDs with identical L_{AC} appears to be the same, driven by the same breakdown mechanism. In Fig. 4(b) and (c), the statistical BV values (when the leakage reaches 5 mA/mm) of GET-SBD1 and GET-SBD2 with

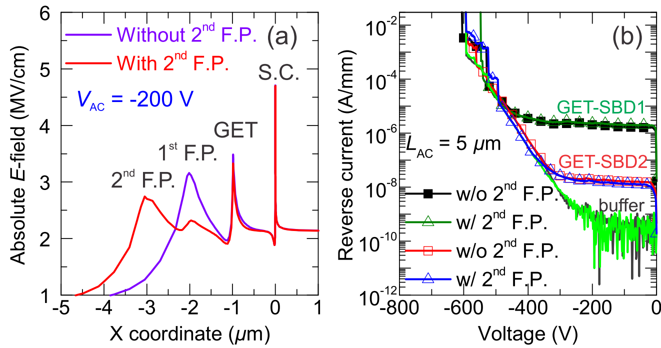

Fig. 5. (a) TCAD simulation of electric field distribution in AlGaN barrier (0.5 nm away from the anode contact) at −200 V. (b) Breakdown characteristics of GET-SBD1 and GET-SBD2 with variation of the second FP, the buffer leakage currents were monitored during the measurements.

L_{AC} variations are shown. With the increase of L_{AC} dimension (from 1.5 to 5 μm), there is a linear increase (∼120 V/μm) of the BV observed in both structures. This BV mechanism is triggered in the AlGaN/GaN active layers in the vicinity of the anode contact, where a peak electric field is present. A further increase of L_{AC} dimension from 5 to 10 μm, however, does not lead to a further enhancement of BV. This is due to the buffer breakdown in the vertical direction, where the electric field increases vertically as the reverse voltage increases. For GET-SBD with L_{AC} of 5 μm, the diode shows excellent performance for 200-V applications. Further buffer design and optimization are needed to boost the buffer BV allowing for higher voltage applications of the diode.

In Fig. 5(a), the electric field distribution in the AlGaN barrier (0.5 nm away from the contact) was simulated in TCAD for GET-SBD with a variation of the second FP. The electric field is more uniformly distributed at the access region; however, the peak electric field at the Schottky contact (SC) does not change with an implementation of the second FP structure. In Fig. 5(b), the breakdown characteristics of GET-SBD1 and GET-SBD2 (L_{AC} of 5 μm) are presented for devices with and without second FP. The buffer leakage currents were monitored simultaneously during the measurements. It is seen that the leakage value prior to breakdown is independent of the second FP for GET-SBD1 and GET-SBD2. This can be explained by the TCAD simulation in Fig. 5(a), which shows an unchanged peak E-field at the anode edge. When reverse voltage exceeds 400 V, the buffer leakage becomes more dominant than the leakage of the diode. It further confirms that the buffer breakdown of the GET-SBD is the limiting factor for its high-voltage operations.

Multifinger GET-SBD power diodes with 10-mm anode width [layout is shown in Fig. 6(a)] have been characterized with the substrate grounded. The temperature-dependent OFF-state characteristics of GET-SBD1 and GET-SBD2 are shown in Fig. 6(b). The statistical leakage current (at V_R of −200 V) at 25 °C and 150 °C for GET-SBD1 and GET-SBD2 power diodes are presented in Fig. 6(c) and (d), respectively. These results show a good yield of the power diodes, and the optimized GET-SBD2 demonstrates a leakage current of 1.3 μA at 25 °C and 3.8 μA at 150 °C with very weak temperature dependence. This indicates that

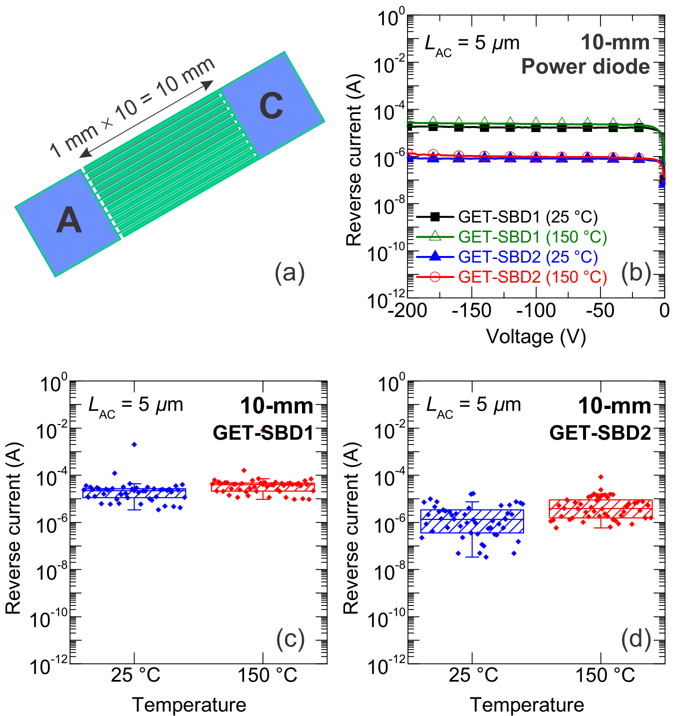

Fig. 6. (a) Layout of 10-mm multifinger GET-SBD. (b) Typical OFF-state characteristics of GET-SBD1 and GET-SBD2 power diodes measured at 25 °C and 150 °C. The statistical leakage values of GET-SBD1 and GET-SBD2 (at 25 °C and at 150 °C) are shown in (c) and (d), respectively.

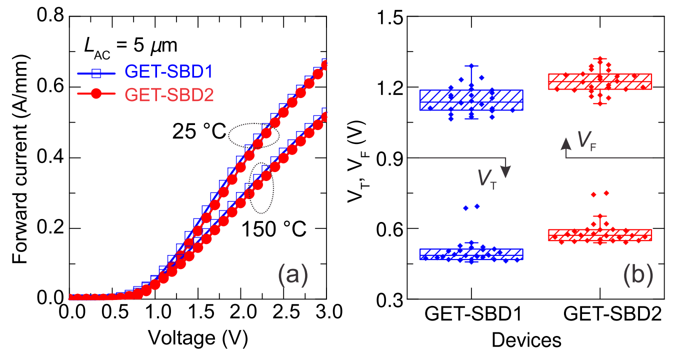

Fig. 7. (a) Typical forward characteristics of GET-SBD1 and GET-SBD2 at both 25 °C and 150 °C. (b) Statistical plot of turn-ON voltage V_T (at forward current of 1 mA/mm) and forward voltage V_F (at forward current of 100 mA/mm) for GET-SBD1 and GET-SBD2 at 25 °C.

our optimized GET-SBDs are promising for high-temperature and high-power applications where a low leakage current is required.

B. Forward Current in GET-SBD With PVD TiN and IMP TiN

The typical forward characteristics of GET-SBD1 and GET-SBD2 at both 25 °C and 150 °C are presented in Fig. 7(a). The statistical values of turn-ON voltage V_T (at forward current of 1 mA/mm [6], [10], [20]) and forward voltage V_F (at forward current of 100 mA/mm) for GET-SBD1 and GET-SBD2 are shown in Fig. 7(b). The forward voltage defined here combines the effect of the turn-ON voltage and the on-resistance of the diode, which can be a good operating

TABLE II
TEMPERATURE-DEPENDENT LEAKAGE (AT V_{ac} OF −200 V) BENCHMARKING OF Si, SiC, AND LATERAL GaN POWER DIODES

Device	Forward voltage (at 25 °C) at 1 A	I_{OFF} (25 °C)	I_{OFF} (150 °C)	I_{OFF} (150 °C)/I_{OFF} (25 °C)	Substrate cost per cm^2 [21]
GaN Diode (This work)	1.20	1.3	3.8	2.9	~$ 0.08
Si Diode (1N4935)	1.05-1.20	0.1	200	2000	~$ 0.08
SiC Diode (Ref. [22])	1.20	0.01	0.1	10	~$ 6

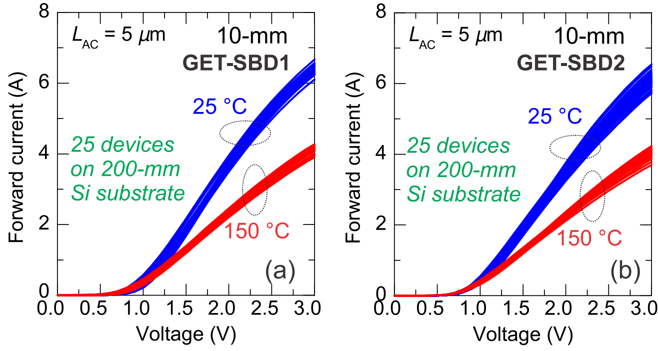

Fig. 8. Forward characteristics of (a) GET-SBD1 power diodes and (b) GET-SBD2 power diodes measured at 25 °C and 150 °C. The results show high yield and good uniformity over 200-mm silicon wafers.

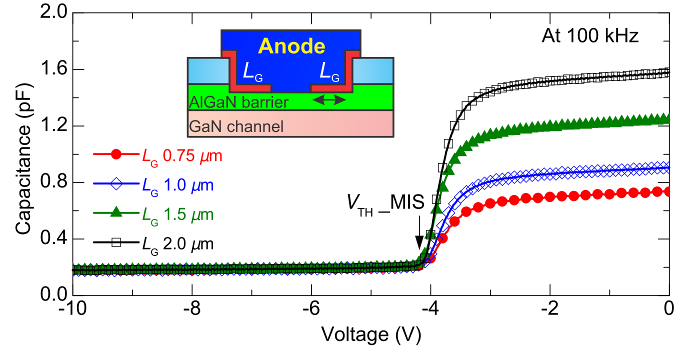

Fig. 9. C–V measurements on GET-SBD2 with L_G variations measured at 100 kHz. The inset schematic structure shows the anode region of the GET-SBD.

point of the diode. The median values of V_F for GET-SBD1 and GET-SBD2 are 1.14 and 1.22 V, respectively. Though the anode metal IMP TiN has a higher ϕ_m, no severe degradation of ON-state characteristics of GET-SBDs is observed. By using the formula describing the thermionic emission mechanism [23], the apparent SBH for GET-SBD1 and GET-SBD2 can be extracted to be 0.59 and 0.68 eV, respectively. The ideality factor values are 1.30 and 1.23 for GET-SBD1 and GET-SBD2, respectively. Besides the process of the injection of majority carriers over the Schottky barrier, there might be other current transport mechanisms (i.e., tunneling, trap-assisted tunneling, etc.) contributing to the ON-state currents [23].

In Fig. 8(a) and (b), the statistical forward characteristics (at 25 °C and 150 °C) of 25 power diodes with 10-mm anode width are presented for the GET-SBD1 and GET-SBD2 architectures. A high forward current of ~4 A (at 2 V) at 25 °C for both GET-SBD1 and GET-SBD2 power diodes is demonstrated, together with a low leakage current shown in Fig. 6. This statistical evaluation confirms that the GET-SBD architecture with IMP TiN as the anode metal shows excellent performance with low leakage and high forward currents which has been demonstrated on 10-mm power diodes with high yield and good uniformity over a 200-mm silicon wafers.

In Table II, a comparison of the temperature-dependent leakage (at −200 V) of Si, SiC and GaN power diodes is shown. The forward voltage to deliver 1 A for three diodes is similar. The SiC diode shows the lowest leakage at both 25 °C and 150 °C. However, the substrate cost is around 2 orders of magnitude higher than Si and GaN-on-Si diodes. A clear advantage of the GaN diode (GET-SBD2) compared with Si diode lies in its weak temperature-dependent leakage.

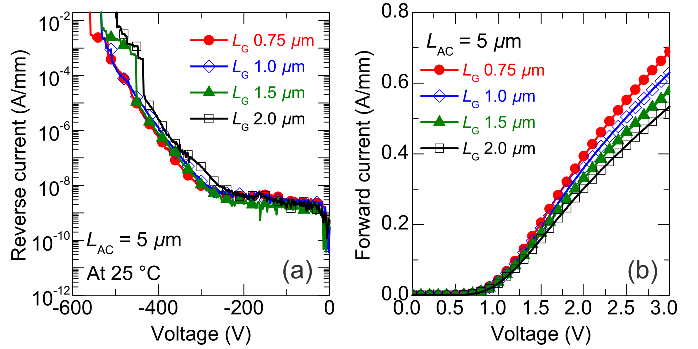

Fig. 10. Typical (a) OFF-state and (b) ON-state characteristics of the GET-SBDs with different L_G dimensions.

Our Au-free GET-SBD power diode with low leakage and high forward currents demonstrates to be a promising candidate for low-cost and high-performance power electronics.

C. L_G Scaling

The gated edge termination (with lateral dimension L_G) in GET-SBD allows for the redistribution of the electric field and the pinching-off of the 2DEG channel, thus low leakage current has been obtained. It is important to note that the dimension of L_G contributes to the capacitance and the ON-state resistance. As shown in Fig. 9, the capacitance–voltage (C–V) measurements have been performed at 100 kHz on GET-SBD2 with different L_G. By scaling down L_G, the capacitance reduces linearly resulting in a more compact configuration. This can potentially reduce the cost and allows for the improvement of ON-state characteristics in GET-SBD2.

In Fig. 10(a) and (b), typical OFF-state and ON-state characteristics of GET-SBD2 (with L_{AC} of 5 μm) with different

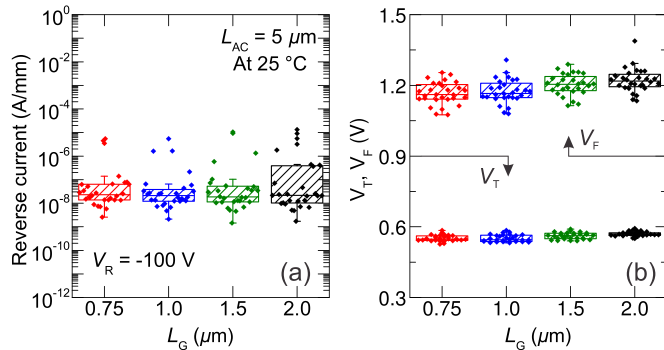

Fig. 11. (a) Statistical plot of leakage current at V_R of −100 V. (b) Statistical values of V_T and V_F for GET-SBDs with a variation of L_G dimensions.

L_G are shown. The leakage characteristics of GET-SBDs show no degradation by scaling down L_G, while an improvement in forward characteristics is observed [shown in Fig. 10(b)] due to reduced series resistance. The statistics of leakage and ON-state voltages are presented in Fig. 11(a) and (b), respectively. By scaling down L_G from 2 to 0.75 μm, the leakage current is invariant and maintains a low value. From the statistics of ON-state voltages, the turn-ON voltage does not change with L_G. A slight improvement of forward voltage is shown in Fig. 11(b). The median value of the forward voltage reduces from 1.22 V to 1.16 V by scaling down the L_G from 2.0 μm to 0.75 μm.

From the results shown in Fig. 11, a leakage current of ~10.0 nA/mm and a forward voltage of 1.16 V have been achieved in GET-SBD2 (with IMP TiN) with L_G of 0.75 μm. Shrinking L_G allows for further optimization of the ON-state characteristics and a more compact design for further cost reduction of Au-free GaN-on-Si technology.

D. Benchmarking of Leakage Versus Forward Voltage, BV Versus $R_{ON,SP}$

In this section, we firstly benchmark earlier reported AlGaN/GaN lateral SBDs and this work (both Au-free and Ni/Au-based technologies) in terms of leakage current (at V_R of −200 V, leakage value from [13] was taken at −127 V) and the forward voltage (at forward current of 100 mA/mm). As shown in Fig. 12, most of the reported AlGaN/GaN SBDs were fabricated using Ni/Au or Pt-based anode metal stacks, which are not compatible with the Si-based processing lines. Our Au-free AlGaN/GaN GET-SBDs with the optimized TiN metal show low leakage current of ~10 nA/mm, which shows competitive performance over most reported data. By scaling down the L_G parameter, the forward voltage can be further reduced without degradation of OFF-state characteristics. This work, to the best of our knowledge, leads to lateral AlGaN/GaN SBDs with the state-of-the-art performance in terms of combined low leakage and low forward voltage. Moreover, excellent characteristics have been demonstrated on power diodes with good yield and uniformity (at both 25 °C and 150 °C) on 200-mm silicon substrate and realized by fabrication in a CMOS-compatible process line.

In Fig. 13, the benchmark plot of BV versus $R_{ON,SP}$ for lateral AlGaN/GaN SBDs on Si and SiC substrates is shown.

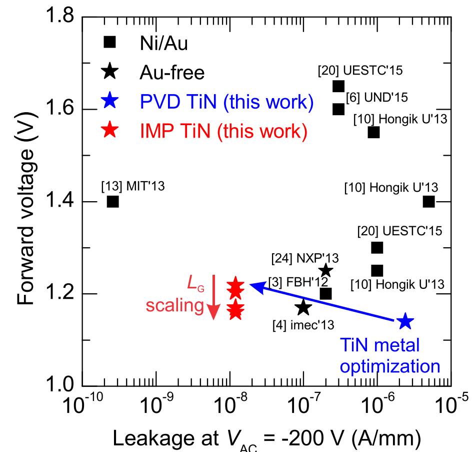

Fig. 12. Benchmarking the leakage current and forward voltage of lateral AlGaN/GaN Schottky diodes with Ni/Au and Au-free technology.

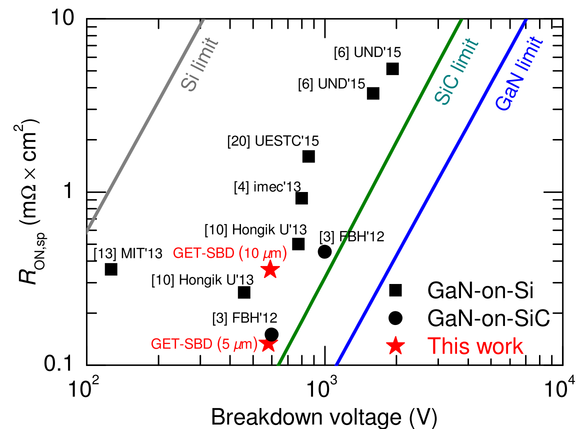

Fig. 13. Benchmarking the BV and specific on-resistance of lateral AlGaN/GaN on silicon and SiC substrate.

The high-performance GET-SBD with L_{AC} of 5 μm demonstrates a power FOM ($BV^2/R_{ON,SP}$) as high as 2.5 GW/cm^2. However, GET-SBD with L_{AC} of 10 μm did not show further increase of BV due to the limitation from the buffer.

IV. Conclusion

This paper optimizes the leakage current of Au-free AlGaN/GaN GET-SBDs by using IMP TiN with a high work-function. A further improvement of the forward voltage is achieved by scaling down the layout parameter L_G without degrading the leakage characteristics, thus a more compact design can be realized for further cost reduction. High-performance AlGaN/GaN GET-SBDs have been demonstrated with 10-mm power diodes, showing high yield and good uniformity with 200-mm silicon substrates. Our GaN power diodes show weak temperature-dependent leakage compared with Si and SiC vertical diodes. The benchmarking of lateral AlGaN/GaN SBDs shows that our optimized Au-free 200-V AlGaN/GaN GET-SBDs are competitive in terms of low leakage current and low forward voltage in comparison with reported data from the literature. To boost the BV of the GET-SBD and allow for higher voltage operation, the design of a more resistive buffer is required.

ACKNOWLEDGMENT

The authors would like to thank H. Tielens for the GIXRD measurements, F. Vleugels for the SEM image analysis, and Prof. E. Simoen and Dr. D. Dictus for the valuable discussions on the work.

REFERENCES

[1] S. L. Selvaraj, A. Watanabe, A. Wakejima, and T. Egawa, "1.4-kV breakdown voltage for AlGaN/GaN high-electron-mobility transistors on silicon substrate," *IEEE Electron Device Lett.*, vol. 33, no. 10, pp. 1375–1377, Oct. 2012.

[2] M. Van Hove *et al.*, "CMOS process-compatible high-power low-leakage AlGaN/GaN MISHEMT on silicon," *IEEE Electron Device Lett.*, vol. 33, no. 5, pp. 667–669, May 2012.

[3] E. Bahat-Treidel *et al.*, "Fast-switching GaN-based lateral power Schottky barrier diodes with low onset voltage and strong reverse blocking," *IEEE Electron Device Lett.*, vol. 33, no. 3, pp. 357–359, Mar. 2012.

[4] S. Lenci *et al.*, "Au-free AlGaN/GaN power diode on 8-in Si substrate with gated edge termination," *IEEE Electron Device Lett.*, vol. 34, no. 8, pp. 1035–1037, Aug. 2013.

[5] J. Hu *et al.*, "Current transient spectroscopy for trapping analysis on Au-free AlGaN/GaN Schottky barrier diode," *Appl. Phys. Lett.*, vol. 106, no. 8, p. 083502, 2015.

[6] M. Zhu *et al.*, "1.9-kV AlGaN/GaN lateral Schottky barrier diodes on silicon," *IEEE Electron Device Lett.*, vol. 36, no. 4, pp. 375–377, Apr. 2015.

[7] D. Christy *et al.*, "Uniform growth of AlGaN/GaN high electron mobility transistors on 200 mm silicon (111) substrate," *Appl. Phys. Exp.*, vol. 6, no. 2, p. 026501, 2013.

[8] B. De Jaeger *et al.*, "Au-free CMOS-compatible AlGaN/GaN HEMT processing on 200 mm Si substrates," in *Proc. IEEE 24th Int. Symp. Power Semiconductor Devices ICs (ISPSD)*, Jun. 2012, pp. 49–52.

[9] J. Hu, S. Lenci, S. Stoffels, B. De Jaeger, G. Groeseneken, and S. Decoutere, "Leakage-current reduction and improved on-state performance of Au-free AlGaN/GaN-on-Si Schottky diode by embedding the edge terminations in the anode region," *Phys. Status Solidi C*, vol. 11, nos. 3–4, pp. 862–865, 2014.

[10] J.-G. Lee, B.-R. Park, C.-H. Cho, K.-S. Seo, and H.-Y. Cha, "Low turn-on voltage AlGaN/GaN-on-Si rectifier with gated ohmic anode," *IEEE Electron Device Lett.*, vol. 34, no. 2, pp. 214–216, Feb. 2013.

[11] Y. Zhang *et al.*, "GaN-on-Si vertical Schottky and p-n diodes," *IEEE Electron Device Lett.*, vol. 35, no. 6, pp. 618–620, Jun. 2014.

[12] Q. Zhou *et al.*, "Over 1.1 kV breakdown low turn-on voltage GaN-on-Si power diode with MIS-gated hybrid anode," in *Proc. IEEE 27th Int. Symp. Power Semiconductor Devices IC's (ISPSD)*, May 2015, pp. 369–372.

[13] E. Matioli, B. Lu, and T. Palacios, "Ultralow leakage current AlGaN/GaN Schottky diodes with 3-D anode structure," *IEEE Trans. Electron Devices*, vol. 60, no. 10, pp. 3365–3370, Oct. 2013.

[14] D. W. Johnson *et al.*, "Challenges of contact module integration for GaN-based devices in a Si-CMOS environment," *J. Vac. Sci. Technol. B*, vol. 32, no. 3, p. 030606, 2014.

[15] S. M. Sze and K. K. Ng, *Physics of Semiconductor Devices*. New York, NY, USA: Wiley, 2006.

[16] J. Hu *et al.*, "Physical origin of current collapse in Au-free AlGaN/GaN Schottky barrier diodes," *Microelectron. Rel.*, vol. 54, nos. 9–10, pp. 2196–2199, 2014.

[17] D. Dictus, D. Shamiryan, V. Paraschiv, W. Boullart, S. De Gendt, and S. Vanhaelemeersch, "Influence of crystallographic orientation on dry etch properties of TiN," *J. Vac. Sci. Technol. B*, vol. 24, no. 5, pp. 2472–2476, 2006.

[18] H. F. Dadgour, K. Endo, V. K. De, and K. Banerjee, "Grain-orientation induced work function variation in nanoscale metal-gate transistors—Part II: Implications for process, device, and circuit design," *IEEE Trans. Electron Devices*, vol. 57, no. 10, pp. 2515–2525, Oct. 2010.

[19] R. Smoluchowski, "Anisotropy of the electronic work function of metals," *Phys. Rev.*, vol. 60, no. 9, pp. 661–674, 1941.

[20] Q. Zhou *et al.*, "High reverse blocking and low onset voltage AlGaN/GaN-on-Si lateral power diode with MIS-gated hybrid anode," *IEEE Electron Device Lett.*, vol. 36, no. 7, pp. 660–662, Jul. 2015.

[21] Y. Zhang *et al.*, "Origin and control of OFF-state leakage current in GaN-on-Si vertical diodes," *IEEE Trans. Electron Devices*, vol. 62, no. 7, pp. 2155–2161, Jul. 2015.

[22] C. Miesner, R. Rupp, H. Kapels, M. Krach, and I. Zverev, "thinQ! Silicon carbide Schottky diodes: An SMPS circuit designer's dream comes true!" White Paper, 2001.

[23] E. Arslan, Ş. Altındal, S. Özçelik, and E. Ozbay, "Dislocation-governed current-transport mechanism in (Ni/Au)–AlGaN/AlN/GaN heterostructures," *J. Appl. Phys.*, vol. 105, no. 2, p. 023705, 2009.

[24] J. J. T. M. Donkers *et al.*, "600 V-900 V GaN-on-Si process technology for Schottky barrier diodes and power switches fabricated in a standard Si-production fab," in *Proc. CS MANTECH Conf.*, 2013, pp. 259–262.

Jie Hu (S'14) received the M.Sc. (*magna cum laude*) degree in nanoscience and nanotechnology from the Katholieke Universiteit Leuven, Leuven, Belgium, in 2012, where he is currently pursuing the Ph.D. degree in electrical engineering.

He has been with the Power and Mixed Signal Technologies Group, imec, Leuven, since 2012. He is currently a Visiting Researcher with the Massachusetts Institute of Technology, Cambridge, MA, USA.

Steve Stoffels received the M.Sc. (*magna cum laude*) degree in applied physics from the University of Eindhoven, Eindhoven, The Netherlands, in 2001, and the Ph.D. degree from the Katholieke Universiteit Leuven, Leuven, Belgium, in 2010.

He is currently a Device Engineer with imec, Leuven, where he is involved in the research and development of high-power GaN technology. He is also acting as a Project Manager for funded projects.

Silvia Lenci received the M.Sc. degree in electrical engineering from the University of Pisa, Pisa, Italy, in 2006, and the Ph.D. degree from the Department of Information Engineering, University of Pisa, in 2010.

She is currently with imec, Leuven, Belgium. Her current research interests include GaN-based high-power electronic devices and sensors.

Benoit Bakeroot received the M.Sc. degree in physics and the Ph.D. degree in electrical engineering from Ghent University, Ghent, Belgium, in 1997 and 2004, respectively.

He joined imec, Leuven, Belgium, in 1998. He has been involved in GaN-on-Si devices since 2010. During his research career, he has used technology computer-aided design for the study of semiconductor devices. He is currently a part-time Assistant Professor with Ghent University.

Brice De Jaeger received the B.S. and M.S. degrees in electrical engineering from Ghent University, Ghent, Belgium, in 1994 and 1997, respectively.

He has been a Research Engineer in different research departments with imec, Leuven, Belgium. He has collaborated in the technology development, integration, and characterization of interconnects and germanium CMOS transistors. His current research interests include GaN technology for power applications.

Marleen Van Hove received the M.S. degree in physics and the Ph.D. degree from the Catholic University of Leuven, Leuven, Belgium, in 1980 and 1985, respectively.

She then joined imec, Leuven. She specialized in GaAs and InP III–V processing from 1986 to 1997. She was responsible for CMOS back-end integration at imec. In 2006, she returned to III–V research, where she is responsible for the development of high-power GaN-switching devices.

Nicolò Ronchi was born in Thiene, Italy. He received the Laurea degree in electronics engineering and the Ph.D. degree from the University of Padua, Padua, Italy, in 2008 and 2012, respectively.

He has been a Researcher with the Power and Mixed Signal Technologies Group, imec, Leuven, Belgium, since 2012. His current research interests include the characterization and reliability analysis of GaN-based semiconductor devices for high-frequency and power-switching applications.

Rafael Venegas received the M.Sc. degree in physics from the University of Chile, Santiago, Chile, in 1976, and the Ph.D. degree in physics from University Joseph Fourier, Grenoble, France, in 1979.

He was with the Chilean Atomic Energy Commission, Santiago, until he became an Associate Professor with the University of Santiago de Chile, Santiago, in 1985. In 2000, he joined the Mixed Signal Technologies Group, imec, Leuven, Belgium.

Hu Liang received the B.Sc. degree in physics from Beijing Normal University, Beijing, China, in 1996, and the M.Sc. and Ph.D. degrees in electronics and computer engineering from The Hong Kong University of Science and Technology, Hong Kong, in 2003 and 2007, respectively.

He has been with the Epitaxial Group, imec, Leuven, Belgium, since 2010, where he is currently a Senior Research Scientist.

Ming Zhao received the M.Sc. degree in material engineering and the Ph.D. degree in material physics from Linköping University, Linköping, Sweden, in 2003 and 2008, respectively.

He joined imec, Leuven, Belgium, in 2008, as a Researcher, where he has been a Senior Researcher since 2012. His current research interests include epitaxy, material characterizations, and device physics of III–N and group IV materials.

Guido Groeseneken (S'81–M'89–SM'95–F'05) received the M.Sc. degree in electrical engineering and the Ph.D. degree in applied sciences from the Katholieke Universiteit Leuven (KU Leuven), Leuven, Belgium, in 1980 and 1986, respectively.

He joined the Research and Development Laboratory, imec, Leuven, in 1987, where he became a fellow in 2007. Since 2001, he has been a Professor with the Department of Electrical Engineering, KU Leuven.

Stefaan Decoutere received the M.Sc. degree in electronic engineering and the Ph.D. degree from Katholieke Universiteit Leuven, Leuven, Belgium, in 1986 and 1992, respectively.

He has been with imec, Leuven, since 1987. In 1998, he became the Head of the Mixed Signal/RF Technology Group with imec. Since 2010, he manages the GaN Power Device technology development, and in 2015, he became the Director of the GaN technology program.